A revised tsunami source model for the 1707 Hoei earthquake and simulation of tsunami inundation of Ryujin Lake, Kyushu, Japan

Takashi Furumura,[1,2] Kentaro Imai,[1,2,3] and Takuto Maeda[1,2]

Received 9 August 2010; revised 5 November 2010; accepted 1 December 2010; published 16 February 2011.

[1] Based on many recent findings such as those for geodetic data from Japan's GEONET nationwide GPS network and geological investigations of a tsunami-inundated Ryujin Lake in Kyushu, we present a revised source rupture model for the great 1707 Hoei earthquake that occurred in the Nankai Trough off southwestern Japan. The source rupture area of the new Hoei earthquake source model extends further, to the Hyuga-nada, more than 70 km beyond the currently accepted location at the westernmost end of Shikoku. Numerical simulation of the tsunami using a new source rupture model for the Hoei earthquake explains the distribution of the very high tsunami observed along the Pacific coast from western Shikoku to Kyushu more consistently. A simulation of the tsunami runup into Ryujin Lake using the onshore tsunami estimated by the new model demonstrates a tsunami inundation process; inflow and outflow speeds affect transport and deposition of sand in the lake and around the channel connecting it to the sea. Tsunamis from the 684 Tenmu, 1361 Shokei, and 1707 Hoei earthquakes deposited sand in Ryujin Lake and around the channel connecting it to the sea, but lesser tsunamis from other earthquakes were unable to reach Ryujin Lake. This irregular behavior suggests that in addition to the regular Nankai Trough earthquake cycle of 100–150 years, there is a hyperearthquake cycle of 300–500 years. These greater earthquakes produce the largest tsunamis from western Shikoku to Kyushu.

Citation: Furumura, T., K. Imai, and T. Maeda (2011), A revised tsunami source model for the 1707 Hoei earthquake and simulation of tsunami inundation of Ryujin Lake, Kyushu, Japan, *J. Geophys. Res.*, *116*, B02308, doi:10.1029/2010JB007918.

1. Introduction

[2] Great interplate earthquakes have occurred at the Nankai Trough at a recurrence interval of approximately 100 to 150 years due to the subduction of the Philippine Sea plate beneath southwestern Japan. The Nankai Trough extends from Suruga Bay to the Hyuga-nada. Its total length is approximately 800 km. The history of Nankai Trough earthquake occurrences can be traced through 11 events, beginning with the Hakuho Nankai earthquake in AD 684 [e.g., *Ishibashi*, 2004; *Ando*, 1975]. The earthquake occurrence pattern can be characterized by three fault segments: the Nankai, the Tonankai, and the Tokai, from west to east. The fault rupture pattern is described as either simultaneous or individual ruptures of each earthquake segment.

[3] Figure 1 illustrates the Nankai Trough earthquake occurrence pattern for three recent events, the 1944 Tonankai (M7.9) and 1946 Nankai (M8.0) earthquakes, the 1854 Ansei Nankai (M8.4) and Ansei Tokai (M8.4) earthquakes, and the 1707 Hoei earthquake (M8.4). The spread of the source area of the 1944 Tonankai earthquake was rather short and stopped before the Tokai earthquake fault segment. Thus, a Tokai earthquake has not occurred for more than 150 years since the 1854 Ansei Tokai earthquake. Since more than 60 years have been passed since the former earthquake cycle we expect that next earthquake sequence might occur along the Nankai Trough in the next 30 years.

[4] In the recorded history of the Nankai Trough earthquakes the 1707 Hoei earthquake (hereafter called the Hoei earthquake) was the largest shock in modern Japanese history. It killed more than 20,000 people due to its strong ground motion and the tsunami associated with the earthquake [*Usami*, 1996, 2003]. The fault rupture area of the Hoei earthquake has been thought to spread from Suruga Bay to the westernmost end of Shikoku, i.e., the whole extent of the 1854 Ansei Tokai and the 1854 Ansei Nankai earthquake source segments. Therefore, the Hoei earthquake is often referred as a worst case scenario for earthquakes occurring in the Nankai Trough. This source model is often used for assessing earthquake-induced damage expected for future Nankai Trough earthquakes.

[5] The source rupture histories of the recent 1944 Tonankai and 1946 Nankai earthquakes were examined

[1]Center for Integrated Disaster Information Research, Interfaculty Initiative in Information Studies, University of Tokyo, Tokyo, Japan.
[2]Earthquake Research Institute, University of Tokyo, Tokyo, Japan.
[3]Now at Tsunami Engineering Laboratory, Disaster Control Research Center, Tohoku University, Sendai, Japan.

0148-0227/11/2010JB007918

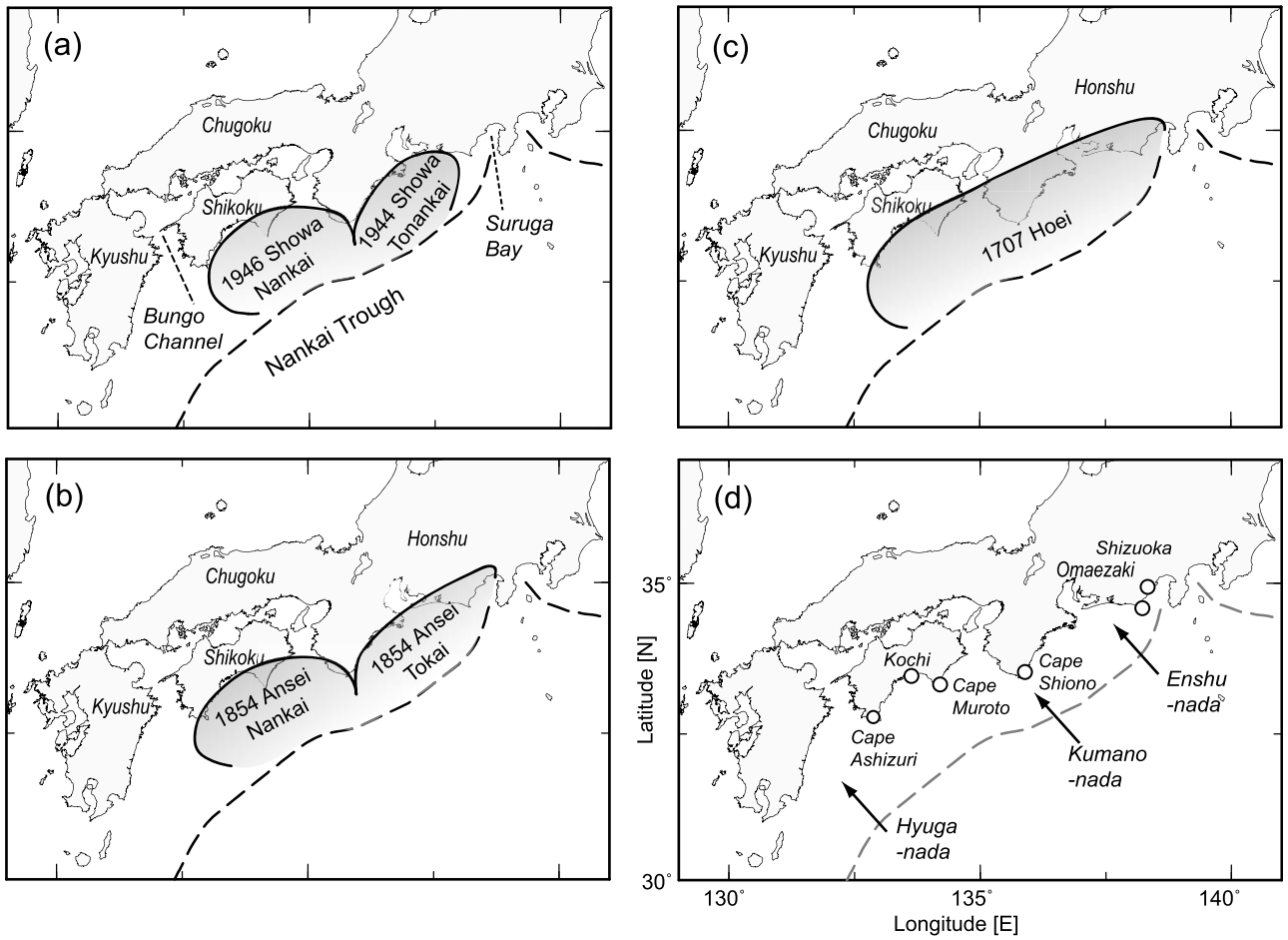

Figure 1. Source rupture areas of recent three Nankai Trough earthquake cycles: (a) the 1944 Tonankai and 1946 Nankai earthquakes, (b) the 1854 Ansei Nankai and Tokai earthquakes, and (c) the 1707 Hoei earthquake. (d) An index map illustrating major place names.

extensively based on the analysis of modern instrumental data, such as tide gauge records of tsunami waveforms [*Aida*, 1981; *Tanioka*, 2001; *Tanioka and Satake*, 2001; *Baba et al.*, 2002, 2006], seismograms of regional strong ground motions and teleseismic waveforms [*Ichinose et al.*, 2003; *Murotani*, 2007; *Yamanaka*, 2004], geodetic data derived from leveling surveys [*Fitch and Scholz*, 1971; *Kanamori*, 1972; *Ando*, 1975; *Ishibashi*, 1981; *Sagiya and Thatcher*, 1999], and combinations of these data [*Satake*, 1993]. Source models of historical events such as the Hoei earthquake, on the other hand, have mostly been deduced from descriptions of earthquake phenomenon in ancient documents such as shaking felt by humans, damage to houses, and visual measurements of tsunami inundation or tsunami runup height. *Ando* [1975] deduced the source model of the Hoei earthquake using various data sets, including the vertical movements of ground surface associated with the earthquake [*Kawasumi*, 1950], the distribution pattern of seismic intensities [*Omori*, 1913], and comparisons between these phenomena and measurements from the recent 1944 Tonankai and 1946 Tokai earthquakes. *Aida* [1981] deduced a source model for the Hoei earthquake based on tsunami data compiled by *Hatori* [1966, 1974] and presented a better source model that explains distribution of the tsunami height along the Pacific coast from Shikoku to Suruga Bay. *An'naka et al.* [2003] modified the source model of *Aida* [1981] and improved the agreement between tsunami simulations and observed tsunami height distributions.

[6] The source model for the Hoei earthquake deduced by *Ando* [1975], *Aida* [1981], and *An'naka et al.* [2003] determined that the source rupture area of this event extends from Suruga Bay to the westernmost end of Shikoku, i.e., the whole extent of the source area of the 1856 Ansei Tokai and the Ansei Nankai earthquakes. However, it should be kept in mind that objective data, such as shaking intensities and tsunami heights in Kyushu, were rather limited at that time and thus, these data may not well incorporated in their analysis. Thus, further supporting evidence is needed to develop a reliable and detailed source rupture history for the Hoei earthquake.

[7] Recently, there have been numerous works reporting geological surveys of earthquake-related lacustrine sediment in seashore lakes along the Pacific coast from Shikoku to Kyushu. These studies endeavor to clarify the tsunami history of the historical and prehistorical Nankai Trough earthquakes [e.g., *Tsukuda et al.*, 1999; *Okamura et al.*, 1997, 2000, 2003, 2004; *Tsuji et al.*, 1998, 2002; *Nanayama and Shigeno*, 2004;

Table 1. Fault Parameters for the 1707 Hoei Earthquake Described by Subfault Segments N1 to N4[a]

Segment	Fault Location (Latitude (°N)/ Longitude (°E))	Length (km)	Width (km)	Depth (km)	Strike (deg)	Dip (deg)	Rake (deg)	Slip (m)
N1	35.120/138.706	120	50	6.4	193	20	71	5.6
N2	33.823/138.235	205	100	4.1	246	10	113	7.0
N3	33.006/136.074	155	100	7.8	251	12	113	5.6
N4	32.614/134.481	125	120	10.1	250	8	113	9.2

[a]After *An'naka et al.* [2003]. The fault location indicates east corner of each subfault.

Komatsubara and Fujiwara, 2007; *Matsuoka and Okamura*, 2009]. Ryujin Lake is one such onshore lake that has tsunami-induced oceanic deposits (hereafter called tsunami lakes), located along the coast of the Hyuga-nada in Kyushu. Ryujin Lake has a thick cover of marine deposits, including coarse-grained sea sands and marine sediments containing oceanic plankton carried by Nankai Trough earthquake. It should also be noted that such tsunami-induced onshore deposits have not accrued regularly in Ryujin Lake due to the Nankai earthquakes that occur every 100 to 150 years, but were only deposited in the 1707 Hoei earthquake, the 1361 Shohei earthquake, and the 684 Tenmu earthquake, which are probably associated with larger tsunamis than the other Nankai earthquakes [*Matsuoka and Okamura*, 2009; *Okamura et al.*, 2004]. Recent findings in the historical documents claim that the height of the tsunami during the Hoei earthquake at the village of Yonouzu, near Ryujin Lake, was more than 10 m, which is very much larger than the tsunamis associated with the 1854 and 1946 events [*Chida et al.*, 2003; *Chida and Nakayama*, 2006].

[8] Recent developments of the Japanese GEONET nation-wide GPS network illustrating the pattern of present ground deformation which is considered to be undergoing recovery process of post-Nankai Trough earthquake. Also, studies on interplate coupling along the Nankai Trough based on the GEONET data [e.g., *Ichitani et al.*, 2010; *Hashimoto et al.*, 2009; *Nishimura et al.*, 1999; T. Hashimoto, http://www.jamstec.go.jp/esc/projects/fy2009/12-hashi.html] reveal an area where strong interplate coupling occurs along the Nankai Trough subduction zone.

[9] Following these new findings and supporting instrumental data, we will reexamine the source model for the Hoei earthquake. Our belief based on detail tsunami simulation is that the source rupture area of the Hoei earthquake extended an additional 70 km eastward to the Hyuga-nada from the westernmost end of Shikoku. Thus, the Hoei earthquake was not a linkage occurrence of the 1854 Ansei Nankai and the Ansei Tokai earthquakes but a much larger event. Similar discussion on the possible extension of the Hoei earthquake source area was also discussed by *Harada and Ishibashi* [2006] based on tsunami simulation. Our new source model with the source rupture area extended to the Hyuga-nada explains the large tsunami observed in Kyushu more consistently than previous models. The tsunami inundated Ryujin Lake, acting together with subsidence of the coastline associated with the earthquake is also explained by the new source model very effectively.

[10] In section 2, we first simulate the tsunami and ground deformation patterns from the Hoei earthquakes to show the applicability and limitations of the current source model of, e.g., *An'naka et al.* [2003]. We compare the simulation results with observed heights of the tsunami along the Pacific coast of the Nankai Trough, especially from western Shikoku to Kyushu [*Hatori*, 1974, 1985; *Murakami et al.*, 1996]. We then reexamine the source model of the Hoei earthquake based on recent objective data derived by the geological and geodetic investigations mentioned above. Finally, we simulate the tsunami runup and inundation of Ryujin Lake using a high-resolution bathymetric model to demonstrate the effectiveness of our new Hoei model in duplicating observed data due to the earthquake and to understand how the tall tsunami generated by the Hoei earthquake transported oceanic sand into Ryujin Lake.

2. Tsunami Simulation for the 1707 Hoei Earthquake

[11] We first conducted tsunami simulation for the Hoei earthquake using a source model of *An'naka et al.* [2003] to examine the effectiveness of the present source model for reproducing observed height of the tsunami along the Pacific coast of the Nankai Trough [*Hatori*, 1974, 1985; *Murakami et al.*, 1996].

2.1. Deformation of the Ground Surface in the Hoei Earthquake

[12] The source model of the Hoei earthquake deduced by *An'naka et al.* [2003] consists of four fault segments (N1 to N4), which extend from Suruga Bay to the westernmost end of Shikoku, a total length of 605 km. The geometry and source parameters of each segment are shown in Table 1.

[13] Figure 2 illustrates the calculated vertical ground deformation due to fault rupture of the N1 through N4 fault segments for the Hoei earthquake, derived following *Mansinha and Smylie* [1971]. Large slips over the shallowly dipping N1 through N4 fault planes over the subducting Philippine Sea plate develop coseismic deformations on the Earth's surface with upheaval and subsidence of several tens of centimeters to meters in height extending along the source rupture area. Such deformations of the ground surface associated with large subduction zone earthquakes are known to produce marine terraces by upheaval and onshore lakes by subsidence. Postseismic deformations of the ground surface during interearthquake cycles gradually resolve such earthquake-induced deformation to a normal level over tens of years. Large ground upheavals of up to 2 m have been confirmed above the shallowest end of the source fault segment on the trench side. Such ground surface upheaval occurs mostly at sea but some can be found on land, including at Cape Muroto, Cape Shiono, and along the coast of Suruga Bay. On the other hand, large surface subsidence

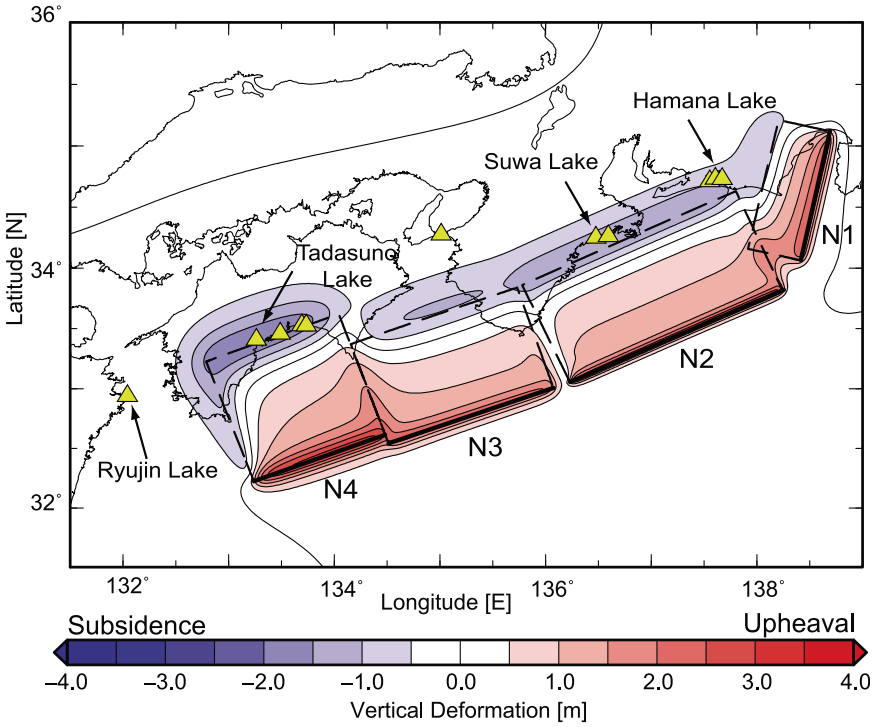

Figure 2. Surface displacement for the 1707 Hoei earthquake calculated using the source model of *An'naka et al.* [2003] with ground surface subsidence (blue) and upheaval (red). The contour interval is 0.5 m. Triangles show locations of the lakes that have tsunami deposits from the Nankai Trough earthquakes.

of as much as 2 m is found widely on land in a narrow belt zone extending from Shizuoka to the westernmost end of Shikoku. Such ground deformations caused by the rupture of the N1 to N4 segments is consistent with the observed ground deformation pattern of the Hoei earthquake compiled by *Kawasumi* [1950], which includes large vertical upheavals of 2 to 2.5 m at Cape Muroto, 1 m at Omaezaki, and subsidence of 2 m at Kochi.

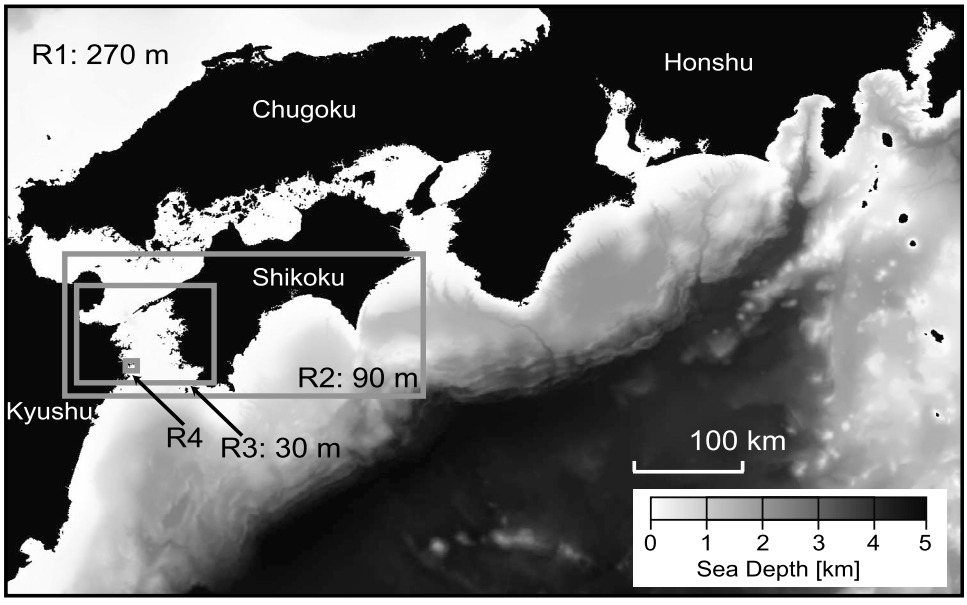

Figure 3. The area of tsunami simulation and mesh configuration connecting gradually from coarser 270 m (R1) to finer 90 m (R2) and 30 m (R3) mesh models. R4 indicates the area of tsunami inundation simulation in the area surrounding Ryujin Lake (Figure 10).

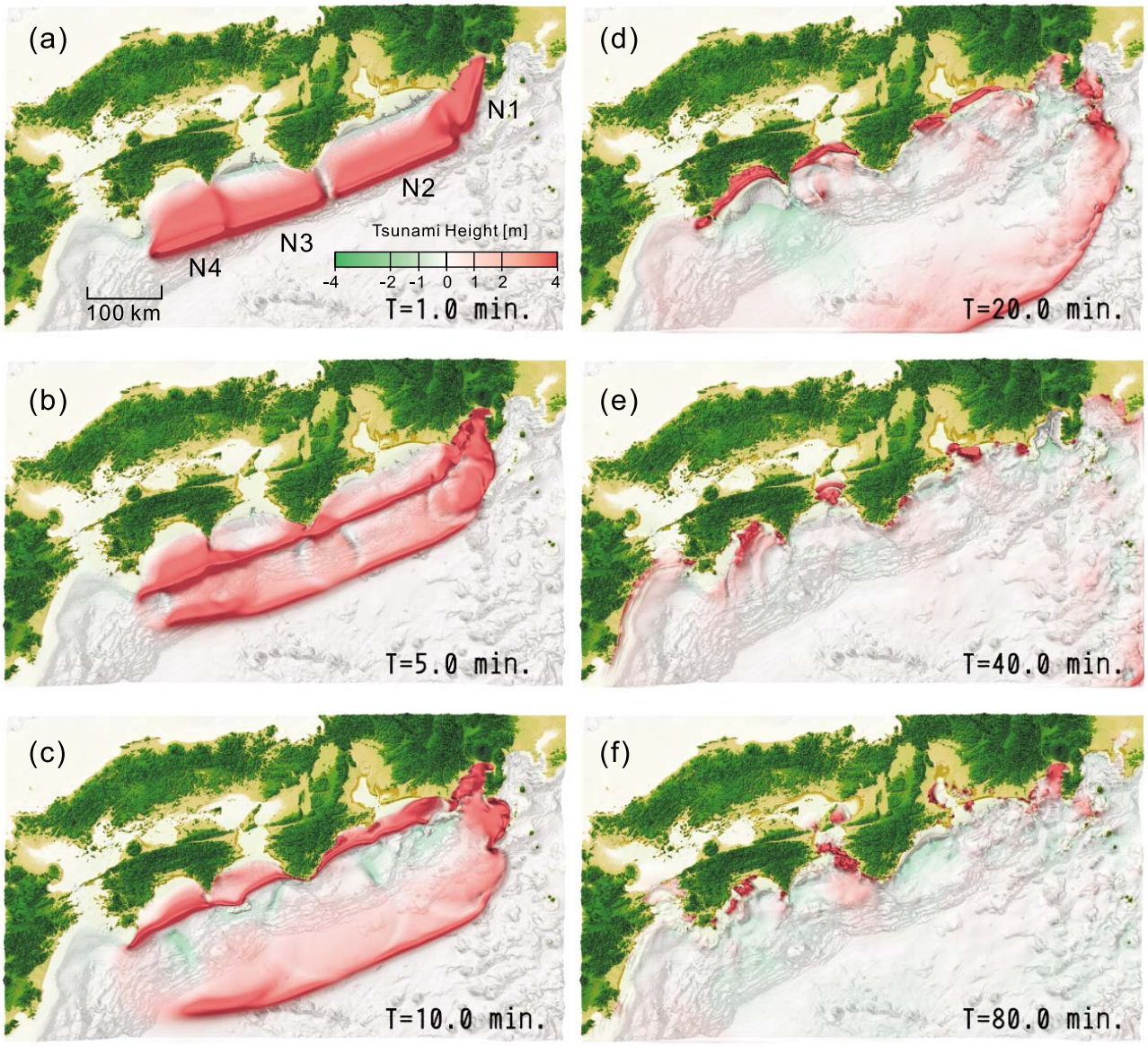

Figure 4. Snapshots of the tsunami associated with the 1707 Hoei earthquake at (a) T = 1.0 min, (b) T = 5.0 min, (c) T = 10.0 min, (d) T = 20.0 min, (e) T = 40.0 min, and (f) T = 80.0 min after the earthquake origin time. Red and blue colors indicate uplift and subsidence of the sea surface, respectively.

2.2. Tsunami Simulation

[14] Using the results of the coseismic ground deformation pattern, we conducted a tsunami simulation for the Hoei earthquake. The area of the tsunami simulation is 540 km by 860 km, which covers the entire Pacific Coast from Honshu to Kyushu where the large tsunami hit during the Hoei earthquake. We used a nested mesh model that connects gradually 30 m, 90 m, and 270 m mesh model to allow efficient simulation of the tsunami in heterogeneous bathymetry (Figure 3). The bathymetric model of each resolution was provided by the Central Disaster Mitigation Council, Cabinet Office, Government of Japan. Subfault segments N1 to N4 of the source model of the Hoei earthquake are divided into small pieces 1 km by 1 km in size. The source rupture is assumed to start in the Kumano Sea off the Kii Peninsula, spreading bilaterally toward Kyushu and Suruga Bay at a rupture speed of Vr = 2.7 km/s. The rupture of each subfault takes 5 s. For simplicity, we assumed that the shape of the initial tsunami on the sea surface is identical to the sea bottom deformation associated with the earthquake. The model of bathymetric and topography model just after the earthquake are modified using resultant vertical ground deformation pattern (Figure 2) due to the earthquake. Then propagation of the tsunami over the sea taking heterogeneous bathymetry into account and tsunami runup on heterogeneous topography are calculated based on a finite difference method (FDM) of a nonlinear, long-wave tsunami model [*Goto and Ogawa*, 1997], assuming Manning's roughness coefficients of 0.025 $m^{-1/3}$ s and 0.04 $m^{-1/3}$ s in the sea and on land, respectively. The computational time

step is set at Dt = 0.6 s to satisfy FDM simulation stability conditions.

[15] Snapshots of tsunami propagation obtained from the simulation of the Hoei earthquake are illustrated in Figure 4 at time T = 1, 5, 10, 20, 40, and 80 min from the time the earthquake started in Animation S1.[1] In Figure 4a (T = 1 min) the development of tsunami above the Hoei earthquake source segment (N1–4) is very striking, with an uplift of the sea surface of approximately 3 m over the Nankai Trough. As time passes, the raised mass of seawater gradually spreads bilaterally as two tsunamis, one propagating toward the seashore and the other to the open ocean at a faster speed. Figure 4b (T = 5.0 min) illustrates two such peaks of elevated sea surface parallel to the trough. Radiation of tsunamis from rectangular fault sources has been confirmed to be very strong in the direction perpendicular to the trough axis, while it is very weak in the direction parallel to the trough. As the tsunami approaches the shore, its speed decreases suddenly and its height increases very drastically. The onshore height of the tsunami, more than 8 m, is several times larger than the height of the initial tsunami above the source area. The later snapshot (Figures 4d and 4e; T = 20 and 40 min) illustrate the arrival of the large tsunami along the Pacific coast from the westernmost end of Shikoku to Hyuga-nada. The tsunami lasts for several tens of minutes after the earthquake. A number of tsunami trains are captured within Tosa Bay (Figure 4f).

[16] Figure 5 illustrates the distribution of maximum simulated tsunami height for *An'naka et al.* [2003] Hoei earthquake source model. From historical records, tsunami heights of 9 m at Tosa Shimizu and Ashizuri Cape and more than 4 m along the coast from Ashizuri Cape to Hyuga-nada are known to have occurred (shown as circles in Figure 5 [*Murakami et al.*, 1996]). The simulated maximum tsunami height along the Pacific coast from Tosa Bay to Suruga Bay generally agrees well with observed tsunami runup during the Hoei earthquake [e.g., *Hatori*, 1974, 1985; *Murakami et al.*, 1996]. However, the height of the simulated tsunami from western Shikoku to Hyuga-nada in Kyushu is less than half of the actual height observed. For example, historical archives document that at Yonouzu village, at the northern end of Hyuga-nada, the tsunami was more than 10 m and killed 18 people [*Chida et al.*, 2003; *Chida and Nakayama*, 2006]. The height of the tsunami during the Hoei earthquake at Yonouzu was several times larger than that experienced during the 1854 Ansei earthquake. Yet the simulated tsunami height at Yonouzu is less than 4 m, which is comparable to the tsunami caused by the 1854 Ansei Nankai earthquake but much shorter than the tsunami experienced with the Hoei earthquake.

3. Revision of the 1707 Hoei Earthquake Source Model

[17] In order to better explain the size of the Hoei earthquake tsunami from Cape Ashizuri to Hyuga-nada, we revised the present source model of the Hoei earthquake developed by *An'naka et al.* [2003] by modifying the structure of the subfault segments off Shikoku based on the findings of a number of recent geodetic and geological investigations of the Nankai Trough.

3.1. Recent Geological Investigations and Tsunami Lakes

[18] Recently, a number of geological experiments of onshore lakes have been carried out to study tsunami-induced deposits on the Pacific coast of central and southwestern Japan in order to better understand the sequence of historical and prehistorical Nankai Trough earthquakes [e.g., *Tsukuda et al.*, 1999; *Okamura et al.*, 1997, 2000, 2004; *Tsuji et al.*, 1998, 2002; *Nanayama and Shigeno*, 2004; *Komatsubara and Fujiwara*, 2007; *Matsuoka and Okamura*, 2009]. Distribution of tsunami lakes such as Hamana Lake at Enshu-nada [e.g., *Okamura et al.*, 2000], Suwa Lake on the Kii Peninsula [e.g., *Tsuji et al.*, 2002], and Tadasuga Lake in Shikoku [e.g., *Okamura et al.*, 2003] are marked by triangles in Figure 2.

[19] Tsunami lakes on the shoreline of the Pacific coast along the Nankai Trough are aligned linearly over the area where large ground subsidence has occurred during Nankai Trough earthquakes (Figure 2). It is thought that ground surface subsidence due to the earthquakes results in particularly deep tsunami inundation on land, which transports sea sand into onshore lakes very effectively. Then, for several tens of years after the earthquake, gradual upheaval of the ground surface occurs and it recovers the subsided ground surface to a normal level and preserves tsunami deposits by protecting from erosion by sea waves or rains for the long periods of time during the interearthquake cycle. The tsunami lakes distributed along the Nankai Trough shoreline lie along a larger zone that subsides during the Nankai Trough earthquakes have developed and preserved in such way. Ryujin Lake, however, recently observed by *Okamura et al.* [2004] at the Hyuga-nada seashore in Kyushu, is not in a location typical of other tsunami lakes in Shikoku and Honshu where large ground subsidence is considered to have occurred during Nankai Trough earthquakes. The pattern of earthquake ground deformation shows that the area of coseismic ground deformation terminates at the westernmost end of Shikoku, approximately 100 km farther east from Ryujin Lake (Figure 2). This implies that the source rupture area of the Nankai subfault segments might not stop at the westernmost end of Shikoku as most source models assume [*Ando*, 1975; *Aida*, 1981; *An'naka et al.*, 2003], but may extend further, to Hyuga-nada.

[20] We therefore examined other findings supporting our hypothesis of an extended source of the Hoei earthquake. The C_{14} age determination for the sedimentation of Ryujin Lake revealed that three sheets of sand layers sandwiched between muddy host sediments were developed during the 1707 Hoei, the 1361 Shohei, and the 684 Tenmu earthquakes [*Okamura et al.*, 2003, 2004]. On the other hand tsunami deposits from the other Nankai Trough earthquakes, which have occurred every 100 to 150 years, do not exist in Ryujin Lake. This implies that unusually large earthquakes associated with larger tsunamis than usual have struck there during the 1707 Hoei, the 1361 Shohei, and the 684 Tenmu earthquakes. The maximum water depth of the lake is approximately 3 m in the center, and a narrow channel or waterway southwest of the lake connects it to the sea. *Okamura et al.* [2003, 2004] noted that the tsunami deposits

[1] Auxiliary materials are available in the HTML. doi:10.1029/2010JB007918.

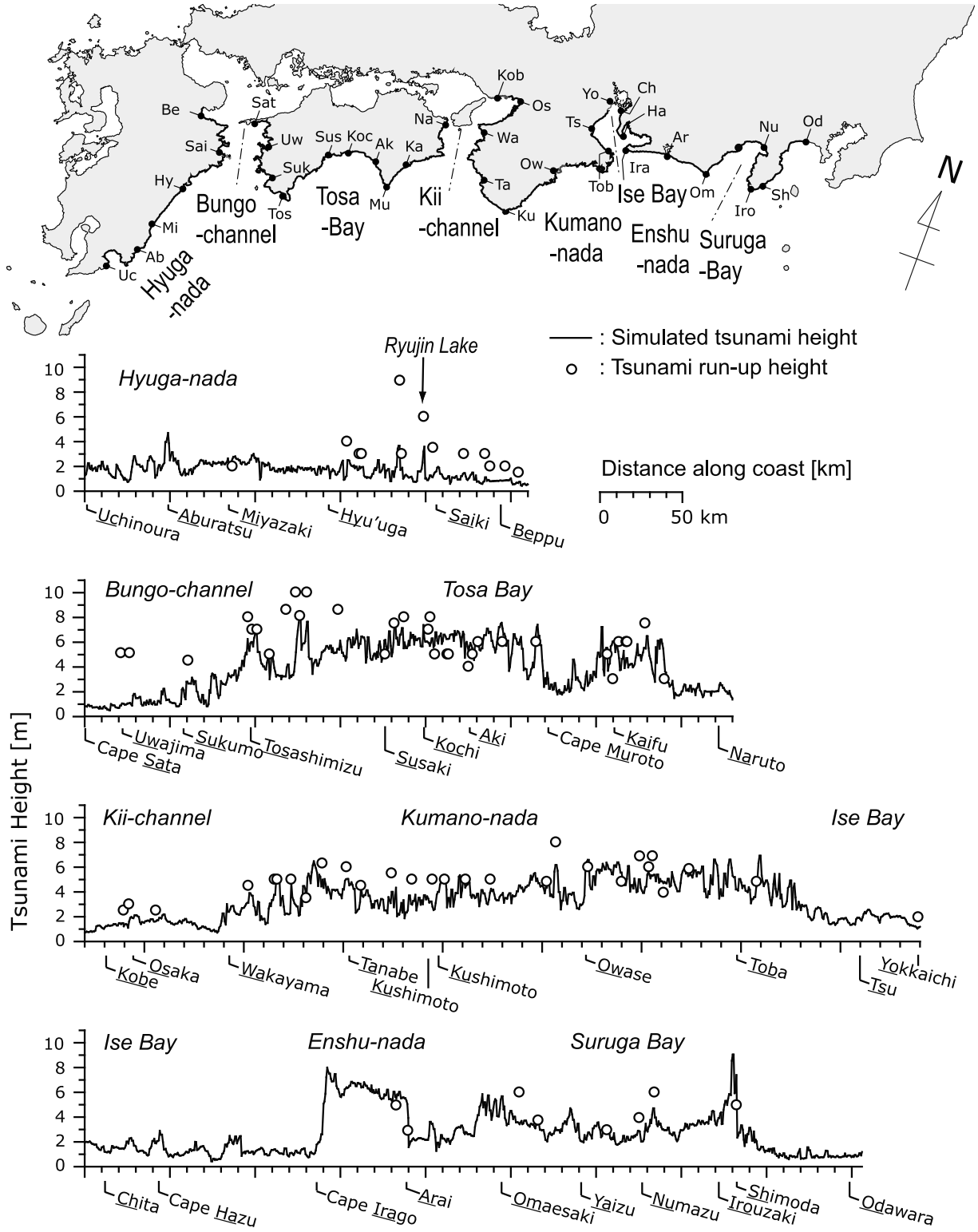

Figure 5. Maximum tsunami height along the Pacific coast of Japan. The map on the top shows the Pacific coastline from Hyuga-nada to Suruga Bay with representative locations. The bottom four plots show the distribution of maximum tsunami height calculated using the simulation of the Hoei earthquake by *An'naka et al.* [2003]. Circles denote observed tsunami heights during the earthquake [*Hatori*, 1974, 1985; *Murakami et al.*, 1996].

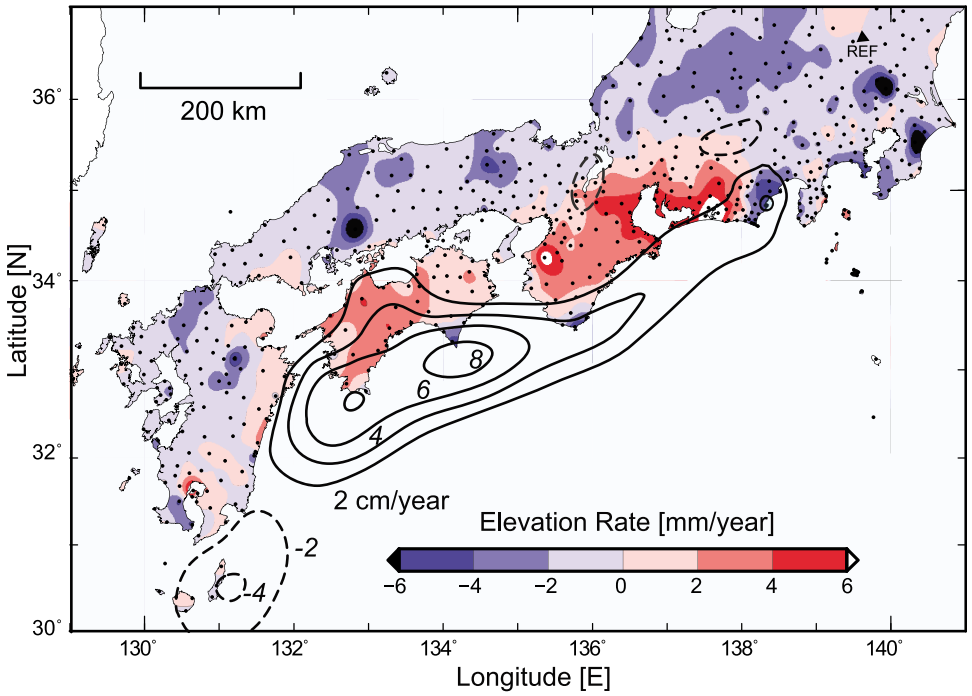

Figure 6. Pattern of average vertical movements of uplift (red) and subsidence (blue) derived using the GEONET GPS data from August 1999 to August 2009 are illustrated by blue-red color scale. The triangle at the top right indicates the reference point used in this analysis. Thick solid and dashed contour lines illustrate slip delay and advance rate at the plate boundary derived by analysis of GPS data by *Hashimoto et al.* [2009] with a contour interval of 2 cm/yr.

are very thick at the southwest side of the lake where the channel connects it to the sea and become thinner toward the center of the lake, implying an another important constraint that tsunami height at the Ryujin Lake was not as tall as overlying beach hill of 10 m surrounding the lake.

3.2. Ground Deformation and Interplate Coupling Pattern Derived From GPS Data

[21] Ten years of data from the nationwide GEONET GPS network illustrates the current pattern of ground deformation (Figure 6). The pattern of vertical ground deformation derived from GEONET data indicates areas where ground upheaval larger than 2 mm/yr has occurred over the past 10 years. A wide upheaval area extends on land from Enshu-nada to Hyuga-nada, roughly covering the area that suffered subsidence due to the Hoei earthquake (Figure 2). Also, sporadic areas of large (>2 mm/yr) ground subsidence appear on land along the shoreline of the Pacific coast such as at Cape Ashizuri, Cape Muroto, Cape Shiono, and Omaezaki. These correspond to ground upheaval areas associated with the Hoei earthquake (Figure 2). This pattern of vertical ground movement is considered to illustrate the process of recovery of ground surface deformation due to the Nankai Trough earthquakes.

[22] If we assume that gentle ground upheaval has continued in the area around Ryujin Lake at a rate of roughly 2 mm/yr until now, the change in ground elevation is estimated to be 60 cm in the past 300 years since the Hoei earthquake in 1707. Because the water level in Ryujin lake is now at mean sea level, it is reasonable to conclude that a large ground subsidence of roughly 60 cm occurred there due to the Hoei earthquake.

[23] We also consulted recent studies on the spatial distribution of interplate coupling rates along the Nankai Trough [e.g., *Hashimoto et al.*, 2009; *Ichitani et al.*, 2010; *Nishimura et al.*, 1999; T. Hashimoto, http://www.jamstec.go.jp/esc/projects/fy2009/12-hashi.html]. Figure 7 illustrates one such result obtained by *Hashimoto et al.* [2009] based on the inversion of horizontal and vertical ground movement data from the GEONET. It shows that an area of strong interplate coupling with high coupling ratios is found from Suruga Bay to Hyuga-nada, more than 100 km beyond the westernmost end of Shikoku which we have considered to be the boundary of the source rupture area for the Nankai Trough earthquake. Similar patterns of plate coupling properties are demonstrated in other studies. *Ichitani et al.* [2010] and *Nishimura et al.* [1999] support the evidence that seismic energy is now accumulating there that may cause a large earthquake in the future.

3.3. Revision of the Hoei Earthquake Source Model

[24] Following these new findings, we revised the source rupture model for the Hoei earthquake and extended the border of the Hoei earthquake source segments of *An'naka et al.* [2003] and others from the westernmost end of Shikoku to Hyuga-nada, where strong interplate coupling has been found by studies using the GEONET data. We worked to match the ground deformation pattern due to the Hoei earthquake and the present ground deformation field shown by the GEONET data, assuming that the significant ground

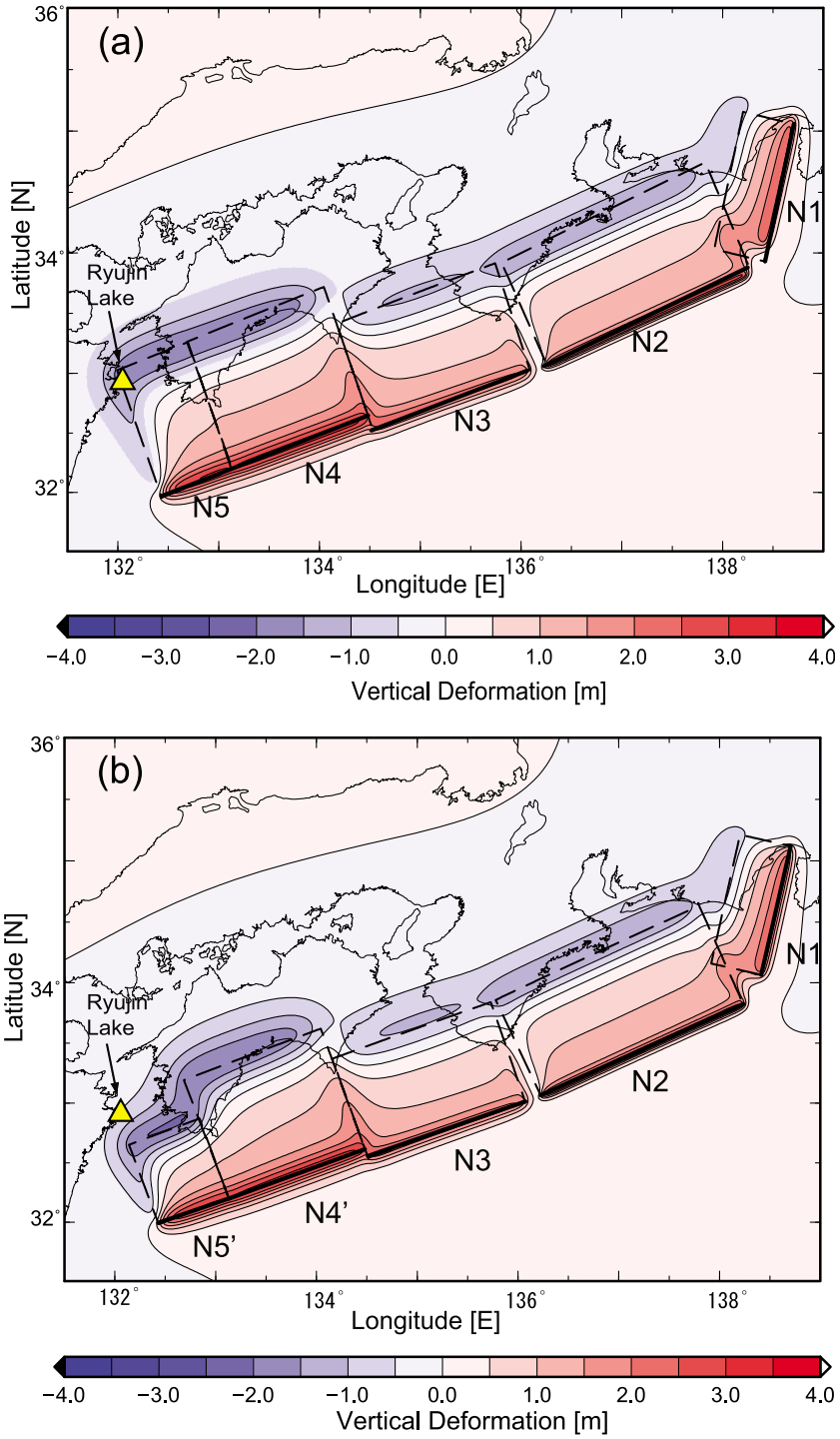

Figure 7. Vertical ground surface deformation derived by the revised 1707 Hoei earthquake source model: (a) an extended source model produced by adding a new N5 subfault segment at the Hyuga-nada and (b) a subfault model with segment N5′ shortened in the direction perpendicular to the trench. Red and blue denote ground surface upheaval and subsidence, respectively. Location of Ryujin Lake is shown by the triangle.

deformation associated with the Hoei earthquake is still influencing the present deformation field.

[25] We first set a 70 km by 120 km subfault segment, N5, on the west of the N4 subfault segment and extended the source rupture area of the Hoei earthquake to Hyuga-nada (Figure 7). Other source parameters, including strike, dip, rake and slip were assumed to be the same as for the N4 subfault segment (Table 2). Figure 8a shows the pattern of ground deformation derived from the new Hoei earthquake source model with subfault segments N1 to N5, demonstrating the extension of the ground subsidence area to Kyushu with maximum ground subsidence of 2 m in a

Table 2. Fault Parameters for the N5, N4′, and N5′ Subfaults of the 1707 Hoei Earthquake

Segment	Fault Location (Latitude (°N)/ Longitude (°E))	Length (km)	Width (km)	Depth (km)	Strike (deg)	Dip (deg)	Rake (deg)	Slip (m)
N5	32.200/133.130	70	120	10.0	250	8	118	9.2
N4′	32.614/134.481	135	120	10.1	250	8	113	9.2
N5′	32.200/133.130	70	80	10.0	250	8	118	9.2

narrow belt from Shikoku to Hyuga-nada. Ryujin Lake is now locating over an area of large (150 cm) ground subsidence. However, the level of ground subsidence in the area around Ryujin Lake derived by the new model is several times larger than we expected (60 cm). Moreover the simulated uplift of 100 cm at Cape Ashizuri is far larger than the uplift observed by *Kawasumi* [1950].

[26] We then modified the geometry of the N5 subfault segment and narrowed it in the direction perpendicular to the trench axis. Also we slightly modified the length of the N4 subfault segment in the direction parallel to the trench axis in order to improve the fitness between synthesized and observed ground deformation pattern reported by *Kawasumi* [1950]. We designated these segments as N4′ and N5′ (Table 2 and Figure 7b). This geometry follows studies on the slow slip events along the Nankai Trough [*Hirose and Obara*, 2005]. An observation of repeatable slow slip events associated with deep tremor activity around the Bungo Channel noted by *Hirose and Obara* [2005] may mean that accumulation of strain energy above the plate boundary is not as strong as would be expected based only on the large plate coupling rate deduced from the GEONET data analysis.

[27] The ground surface deformation pattern derived using subfaults N1 to N5′ is shown in Figure 7b. It agrees well with our expectation of gentle (40 cm) ground subsidence in the area around Ryujin Lake and some subsidence of the ground surface at Cape Ashizuri as noted by *Kawasumi* [1950]. It also corresponds well to the present ground elevation field derived from the GEONET data (Figure 6).

4. Tsunami Simulation Using the New Hoei Earthquake Model

[28] We then conducted a tsunami simulation for the earthquake using the revised source model of the Hoei earthquake (Figure 7b) to see the contribution of the N5′ subfault segment in increasing simulated tsunami height along the coast from Shikoku to Kyushu and in producing tsunami inundation of Ryujin Lake.

[29] Snapshots of tsunami propagation derived by the simulation for the new Hoei earthquake source model with subfault segments N1 to N5′ and the former Hoei earthquake model without segment N5′ are compared in Figure 8 and in Animation S2. Figure 9 shows the maximum simulated tsunami heights for the new model along the Pacific coast of Japan in Shikoku and Kyushu. We will highlight the propagation of the tsunami from Shikoku to Kyushu in order to more clearly examine changes in the tsunami wavefield produced by introducing the new N5′ subfault segment. The comparison clearly demonstrates the development of a larger tsunami with heights of 5 m to over 10 m over a wide area along the Pacific coast from the westernmost end of Shikoku to Hyuga-nada due to the N5′ subfault (Figure 8a). The tsunami radiates very strongly in the direction perpendicular to the Nankai Trough trench axis (Figure 8a; T = 5 min). The height of the tsunami due to the N5′ fault is very strong to spread large tsunami wavefront from Cape Ashizuri to Hyuga-nada (Figure 8a; T = 15 min). As a result, the incremental change in tsunami height due to the N5′ subfault is very significant along the coast from the westernmost end of Shikoku to Hyuga-nada.

[30] In a later snapshot the larger tsunami is radiating into the Bungo Channel and propagating into the Inland Sea of Japan (Figure 8a; T = 30 min), which enhances the height of the tsunami in the Inland Sea. On the other hand, the radiation of the tsunami from the N5′ subfault is very weak in the direction parallel to the trench axis (i.e., southwest to northeast). Thus, the effect of adding the N5′ subfault is only a very minor amplification of the tsunami along the coast from east of Shikoku to Honshu, confirmed by comparing snapshots of Figures 8a and 8b in later time frames (T = 15 and 30 min).

[31] Our tsunami simulation for the new Hoei earthquake model produces a very tall tsunami, 5 to 8 m high at Yonouzu, located approximately 5 km away from Ryujin Lake in Kyushu where the height from the former Hoei earthquake model was less than 2 m (Figure 9). This explains the description in ancient documents of an exceptionally large tsunami approximately 10 m high occurring during the Hoei earthquake [*Chida et al.*, 2003]. The modeled height is much larger than the maximum height of the tsunamis associated with the 1856 Ansei Nankai and 1946 Nankai earthquakes, which were less than 4 m at Yonouzu [*Chida et al.*, 2003; *Chida and Nakayama*, 2006].

[32] The maximum tsunami height along the coast near Ryujin Lake as calculated by the present simulation is 6 m, while it is a maximum of 2 m for the former Hoei earthquake source model without the N5′ subfault segment (Figure 9). Thus, tsunami runup into Ryujin Lake might occur when the Nankai Trough fault rupture extends to Hyuga-nada, but not during events like the 1854 Ansei Nankai and 1946 Showa Nankai earthquakes, in which the fault rupture did not extend past the westernmost end of Shikoku. Our newly simulated tsunami height of approximately 6 m at Ryujin Lake also confirms the interpretation of *Okamura et al.* [2004] that tsunami inundation carrying sea deposits occurs via a narrow channel connecting the sea and lake rather than by overtopping of beach hills that are 10 m high.

5. Simulated Tsunami Inundation of Ryujin Lake

[33] Finally, we conducted a tsunami inundation simulation in order to understand the process whereby the tsunami carried sea sand into Ryujin Lake during the Hoei earthquake,

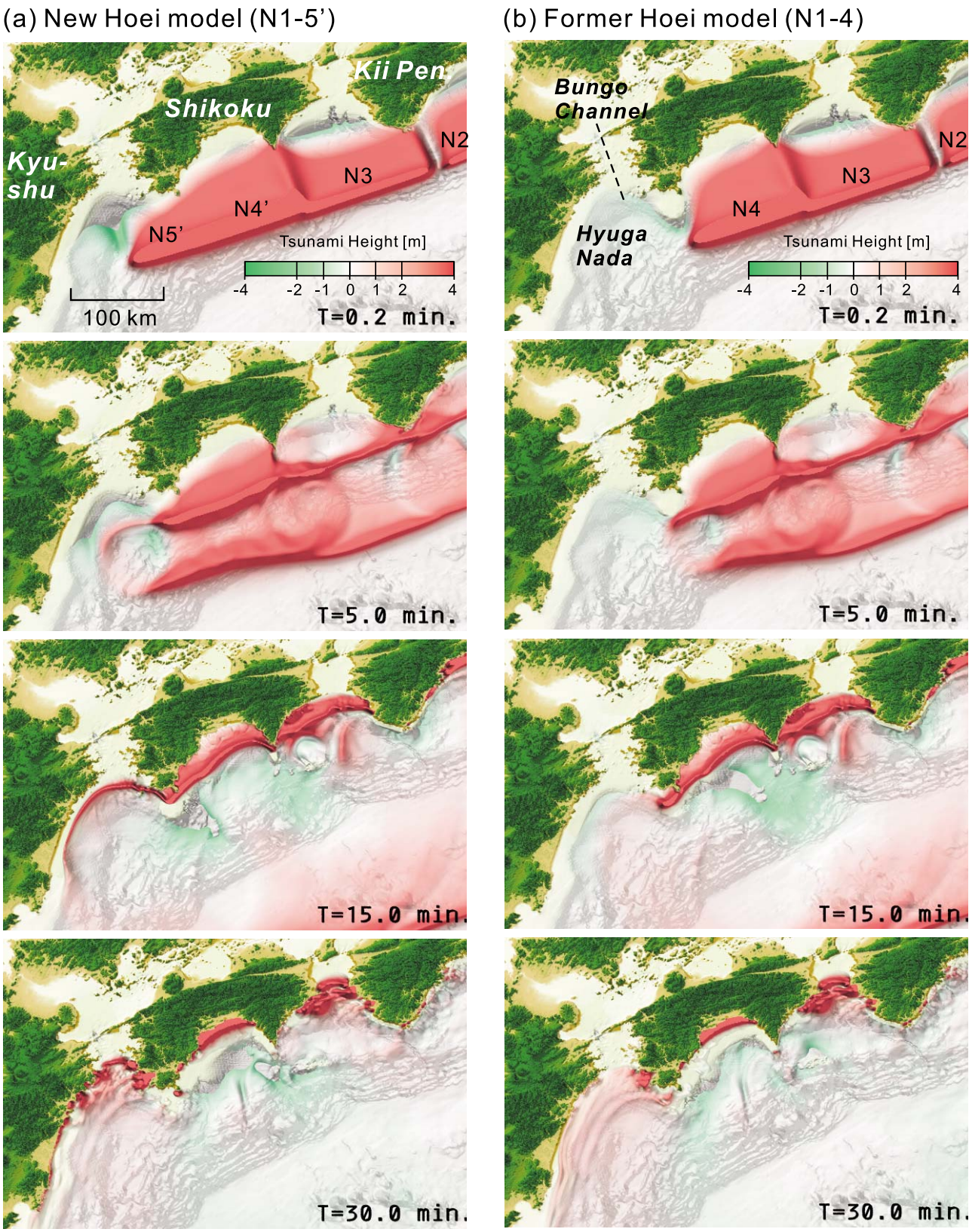

Figure 8. Snapshots of tsunami propagation from the Kii Peninsula to Kyushu derived from simulation at T = 0.2, 5.0, 15.0, and 30.0 min from the earthquake origin time. (a) New Hoei earthquake model with fault segments N1 to N5′ and (b) former Hoei model [after *An'naka et al.*, 2003] with fault segments N1 to N4.

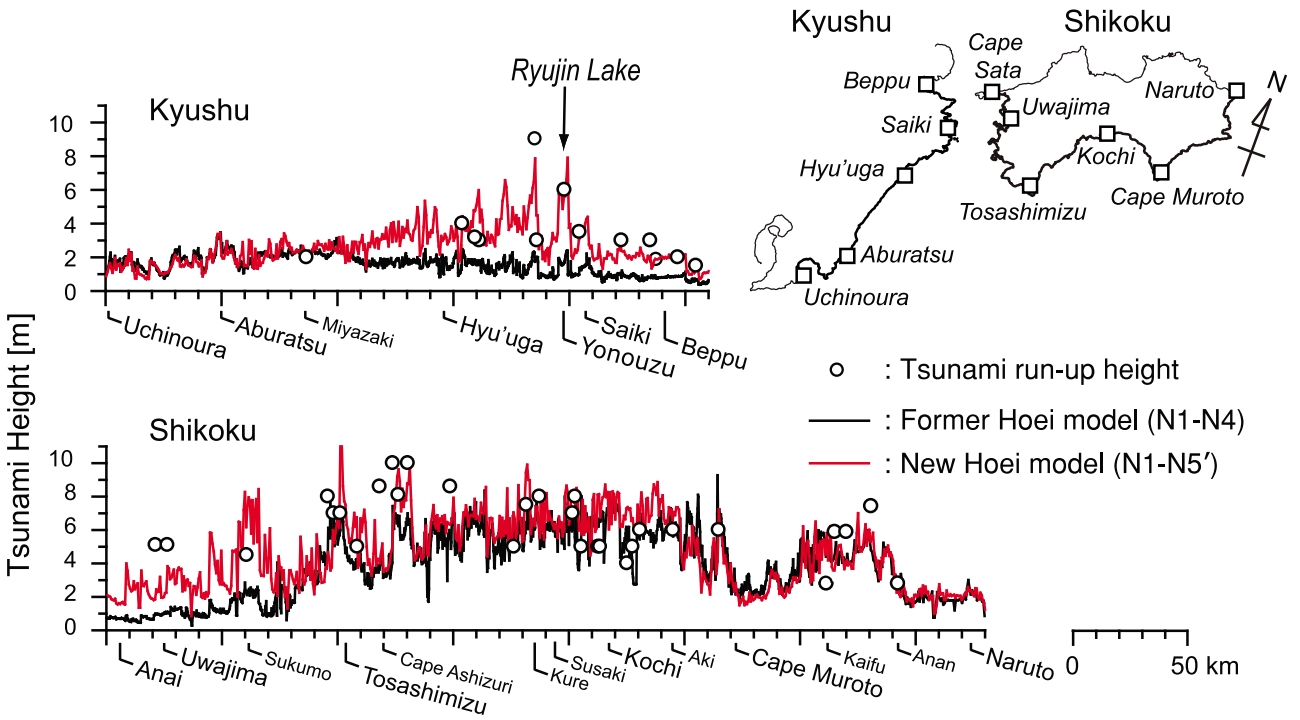

Figure 9. Maximum tsunami height along the Pacific coast of Japan. The map shows the Pacific coastline of Kyushu and Shikoku with representative locations (squares). Also shown are the distributions of maximum tsunami inundation height derived from the simulation of the new Hoei earthquake source model (red lines) and the former Hoei earthquake model (black lines). Circles denote observed maximum tsunami inundation or runup heights during the Hoei earthquake [*Hatori*, 1974, 1985; *Murakami et al.*, 1996].

using the tsunami simulation results from the new Hoei earthquake model described in section 4.

[34] Figure 10 shows the location and topography of the area surrounding Ryujin Lake. Ryujin Lake is surrounded by hills 50 m to 100 m high on the east and south and there is a short beach hill of approximately 10 m on the southwest. There is no river to supply water directly into the lake and inflow and outflow of seawater occur between the lake and the sea during high and low tide, respectively, through a narrow channel connecting it to sea.

[35] The tsunami inundation simulation covers a 200 m by 300 m area around Ryujin Lake. A high-density digital elevation map was constructed on a basis of recent geographical surveys conducted by the Yonouzu Promotion Office, Oita Prefecture. We modified the model to reconstruct the original shoreline structure by removing recent artificial constructions, such as concrete breakwaters and wharfs created by recent shoreline protection projects. The tsunami inundation simulation was conducted using a fine nested mesh model that connects gradually different mesh resolution of 30 m, 10 m, and 3.3 m.

[36] Results from a former large-mesh tsunami simulation, in which height and flux of the tsunami in two horizontal directions at the coast near Ryujin Lake were calculated using the larger (30 m) mesh, were used as inputs in the present tsunami inundation simulation. Before starting the simulation, we subsided the altitude of the simulation model at −60 cm in consideration of the results of the ground deformation simulation shown in Figure 7b.

[37] The results of the tsunami inundation simulation for the new Hoei earthquake model are shown in Animation S3 and in Figure 11 as a sequence of snapshots of the water surface of the Ryujin Lake after T = 14, 19, 24, 29, 34, and 39 min from the start of the earthquake, illustrating the way in which a tsunami with a large flux can inundate Ryujin Lake. In Figure 11b (T = 19 min), the height of the sea surface began to falls as the tsunami wavefront approached. Figure 11c (T = 24 min) shows the seawater gradually inundating the lake through the channel on the right-hand side of the lake. The speed of the seawater at each point is illustrated by red arrows superimposed on the snapshots. These show that the inflow speed from the sea into the lake is a maximum of approximately 6 m/s in the middle of the channel. As the height of the sea surface increases with passing time, the width of the channel grows very dramatically (Figures 11c and 11d; T = 24 and 29 min). This leads to an acceleration of the transmission of seawater into the lake. At this time, the flux of seawater is approximately 1 to 2 m/s at the entrance of the lake and as fast as 5 m/s at the center of the channel. Even though the inflow speed is very large in the channel it should be noted that the speed drops dramatically as it leaves the channel side. This explains the observation of *Okamura et al.* [2003, 2004] that tsunami deposits are very thick at the southwest side of the lake where the channel connects it to the sea and become thinner toward the center of the lake.

[38] At 29 min from the time the earthquake started and about 10 min after the beginning of the lake inundation,

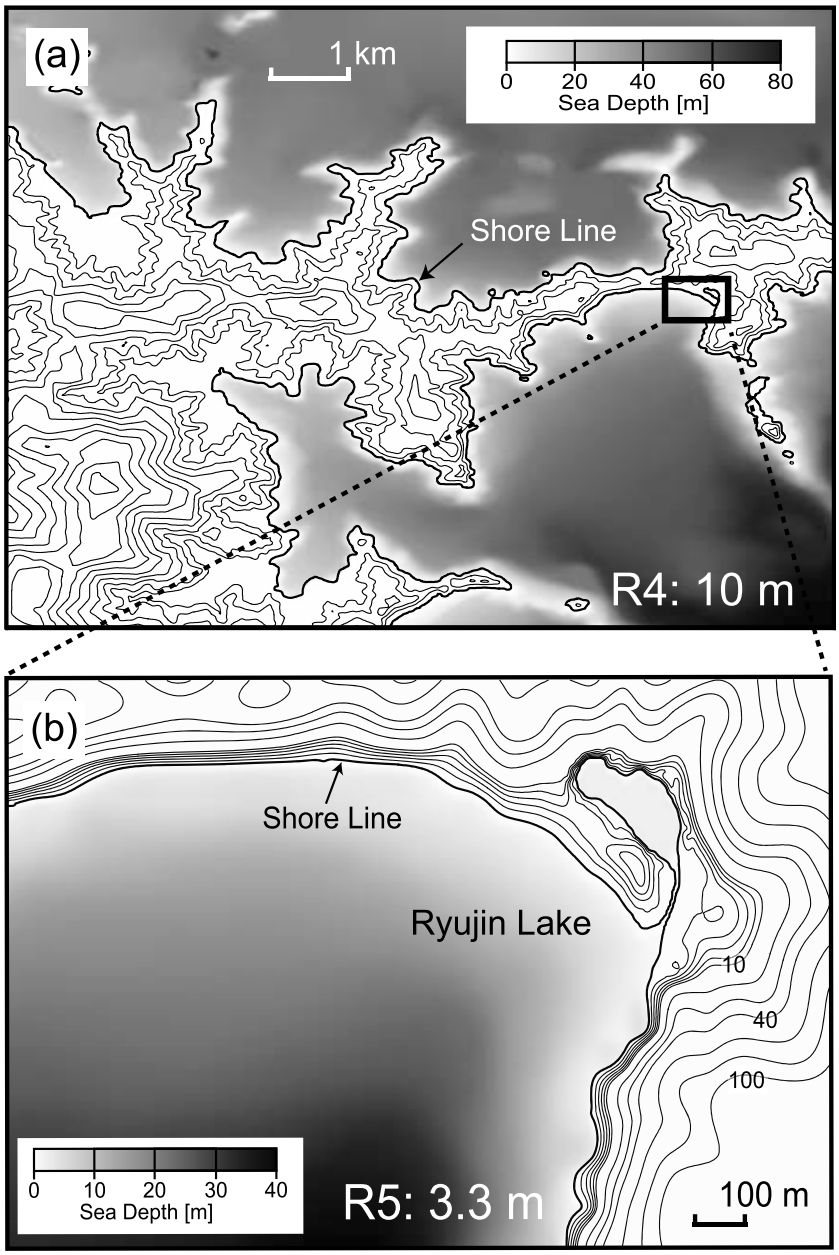

Figure 10. The area of tsunami inundation simulation surrounding Ryujin Lake connecting different mesh resolutions of (a) 10 m and (b) 3.3 m.

flow into the lake almost stops (Figure 11d; T = 29 min). Then the water surface in the lake gradually recedes to mean sea level as the water flows back to the sea through the channel (Figure 11e; T = 34 min). Note that the outflow tsunami current in the channel is very weak, less than 1/5 of the peak tsunami inflow speed (Figure 11e). This implies that the large inflow flux of the tsunami through the channel can carry large masses of sea sand into the lake very effectively, but leaves most of the sand in the lake near the channel when the tsunami goes back to sea.

[39] Figure 12 shows changes of the water height in Ryujin Lake and the flow speed of water in the entrance of the lake connecting to the channel. Just after the earthquake occurs, the height of the surface of Ryujin Lake subsides to 30 cm below mean sea level and then gradually decreases to 40 cm below mean sea level due to the dilatational wave of the tsunami. Then the height of water surface suddenly rises after 20 min from the time of the earthquake, and at 25 min the height of water surface is at its maximum level of approximately 5 m above mean sea level. At this time, a very large (>5 m/s) flux of seawater flows through the center of the channel. It can carry sea sand into the lake very effectively (Figure 12a). A set of tsunami trains with large water fluxes might transport sea sand into the lake very effectively and the relatively slow return current from the lake would leave those sea deposits in the lake.

[40] In order to evaluate the ability of the water flow in the narrow waterway to transport sea sand into the lake through the channel, we calculated the Shields number [e.g., *Takahashi et al.*, 1993], which is an index to specify

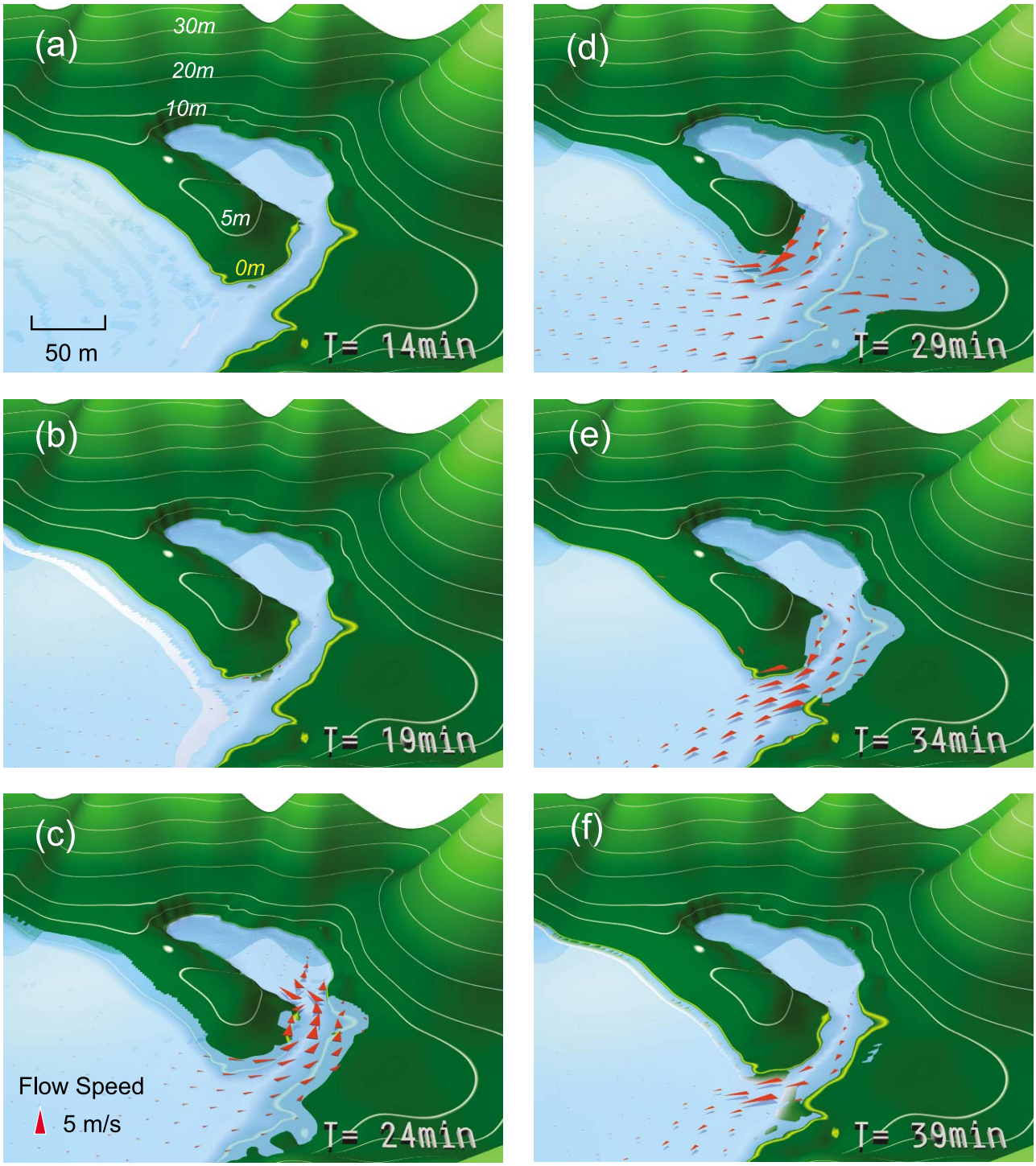

Figure 11. Simulated changes in the water surface during the inundation of Ryujin Lake at (a) T = 14 min, (b) T = 19 min, (c) T = 24 min, (d) T = 29 min, (e) T = 34 min, and (f) T = 39 min from the time the earthquake began. Red arrows denote the speed of the water flow.

strength of transporting capability due to water currents [e.g., *Takahashi et al.*, 1993]. We calculated the Shields number at the middle point of the channel at 2 m deep assuming a Manning's roughness coefficient of n = 0.025 $m^{-1/3}$ s, a sea sand density of r = 1.65 g/cm^3, and median particle diameter for the sea sand of d_{50} = 0.4 mm. These physical constants are assumed from the geology and sedimentation properties of the Ryujin Lake demonstrated by *Okamura et al.* [2004]. The resultant large Shields number, (s > 11), associated with the tsunami's inflow 25 min from the start of the earthquake (Figure 11c), promises that tsunami could efficiently transport sea sand into the lake with very large Shields number of tsunami due to the rupture on the N5′ subfault [see, e.g., *Takahashi et al.*, 1993].

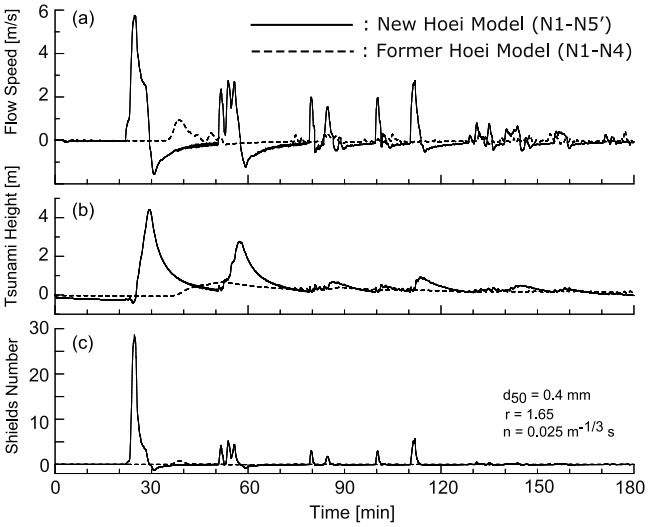

Figure 12. Comparison of tsunami inundation of Ryujin Lake for the new Hoei earthquake model (solid lines) and former earthquake model (dashed lines). (a) Speed of water flow at the entrance of the lake (plus indicates inflow, and minus indicates outflow), (b) water height at Ryujin Lake, and (c) shield numbers showing the power of tsunami transportation.

[41] On the other hand, the water flux in the center of the channel obtained from the former Hoei earthquake model is less than 1 m/s, which is approximately 1/6 of the maximum inflow and almost same as the outflow current speed for the new Hoei earthquake model. Such a slow inflow speed (<1 m/s) and the resultant small Shields number ($s < 1$) indicate that such a tsunami could not transport sea sand into the lake as compare with large Shields number ($s > 11$) of former simulation with the N5′ subfault segment. Therefore, the large tsunami generated by the rupture of the N5′ subfault segment and the swift current it produces in the channel is the only agent that can explain the transport of sea sand into the lake.

[42] The results of tsunami inundation simulation indicate that tsunami-related deposits observed in Ryujin Lake do not occur regularly during Nankai Trough earthquakes but occur during unusually large earthquakes when the fault rupture extends beyond westernmost Shikoku to Hyuga-nada. The Hoei earthquake in 1707 was one such unusually large event, as were the 1361 Shohei and 684 Tenmu earthquakes, evidenced by their ability to deposit tsunami-borne sand in Ryujin Lake [*Matsuoka and Okamura*, 2009; *Okamura et al.*, 2004].

6. Discussion and Conclusion

[43] Of the series of repeating megathrust earthquakes in the Nankai Trough that recur every 100 to 150 years, the Hoei earthquake is considered to be the most damaging, with its linkage of Tokai, Tonankai and the Nankai earthquakes, and fault ruptures extending from Suruga Bay to the westernmost end of Shikoku, about 600 km in length [*An'naka et al.*, 2003].

[44] However, the recent discovery of the tsunami lakes in Kyushu (Ryujin Lake) with their thick cover of tsunami-induced deposits caused by the Hoei earthquake has overturned our understanding. The existence of the tsunami lakes in Kyushu was not well explained by the expected ground deformation pattern produced by the former Hoei earthquake source model where the fault rupture stopped at the westernmost end of Shikoku, not extending to Hyuga-nada. The source model also failed to explain the larger tsunami experienced during the Hoei earthquake from Cape Ashizuri to Hyuga-nada as compared with the tsunami associated with the 1854 Ansei Nankai earthquake.

[45] Actually, the source model of *An'naka et al.* [2003] which is described by four (N1–N4) panels of subfaults might be too simple to demonstrate complicated source rupture history of the Nankai Trough earthquake which should be described by rupture above the subducting Philippine Sea plate and landward dipping splay branch from the plate interface. Such splay faults along the Nankai Trough have recently been imaged with multichannel seismic experiments [e.g., *Moore et al.*, 2007; *Strasser et al.*, 2009], and it is considered to be contributing develop additional tsunami and localized ground deformation above the splay faults during the earthquakes [e.g., *Cummins and Kaneda*, 2000; *Cummins et al.*, 2001]. However, these effects on amplifying tsunami subsides ground surface at Ryujin Lake in Kyushu would be very minor due to larger distances, and most tsunami developed by the splay fault propagates toward rectangular direction of the Trough axis but not to Kyushu. In order to improve tsunami height and ground subsidence in Kyushu, we have to modify source model more drastically.

[46] An inferred property of the present crustal deformation pattern illustrated by the GEONET GPS measurements and a number of studies on interplate coupling along the Nankai Trough subduction zone based on the GPS data [*Hashimoto et al.*, 2009; *Ichitani et al.*, 2010; *Nishimura et al.*, 1999] indicate that Hyuga-nada may also be in the area of the Nankai Trough earthquake nucleation zone. Following these new geological and geodetic findings, we revised the source model of the Hoei earthquake which had described by four subfault segments (N1 to N4) by introducing a new N5′ subfault segment on the western side of Nankai earthquake segment (N4). We succeeded in explaining development of the large tsunami from Cape Ashizuri to Hyuga-nada with maximum tsunami heights of 5 to 10 m that attack along the Pacific coast from the westernmost end of Shikoku to Hyuga-nada. This agrees with the heights of tsunamis observed along the Pacific coast from Cape Ashizuri to Hyuga-nada during the Hoei earthquake [*Hatori*, 1974, 1985; *Murakami et al.*, 1996] very consistently. The tsunami runup into Ryujin Lake estimated by the tsunami inundation simulation using a high-resolution bathymetry model demonstrates the process whereby a large flow of seawater with a large difference in inflow and outflow speeds can transport and deposit sea sand into the lake near the inflow channel very effectively.

[47] In the Hyuga-nada region a relatively large (M6.5–7.5) interplate earthquakes have occurred frequently at interval approximately 20–30 years. For example, recent events are in 1939 (M6.5), 1941 (M7.5), 1961 (M7.0), 1968 (M7.5), and in 1987 (M6.6). The source rupture areas of these events were almost concentrated in the south half part of Hyuga-nada [e.g., *Yagi and Kikuchi*, 2003; *Yoshioka*,

2007], and there was no overlap with the area of our N5′ subfault segment which extends to north half part of Hyuga-nada. Thus, the area of the N5′ subfault is now a seismic gap since the Hoei earthquake in 1707. It is expecting that the rupture of the N5′ subfault segment sometimes occurs by linkage of the N4 Nankai earthquake segment but it does not occurs independently.

[48] The extension of the source rupture area from westernmost Shikoku to Hyuga-nada would produce increased shaking in Kyushu. Exactly what the intensity was in Kyushu in 1707 is unclear; we are unaware of any historical documents that permit a meaningful comparison of intensities of the 1707 and 1856 earthquakes. Further effort is needed to establish the shaking intensity in Kyushu in 1707. In the present paper, we have focused mainly on the significance of the elongation of the Hoei earthquake source rupture to Hyuga-nada in terms of the strengthening of tsunami height and onshore tsunami runup. However, further studies evaluating shaking intensity such as, e.g., based on the FDM simulation of ground motion is needed to completely understand earthquake-related disasters associated with the Nankai Trough earthquakes. We hope recent investigation of high-resolution geological and geophysical experiments will provide high-density reliable subsurface structure model as well as heterogeneous source rupture model. Steadily improving high-performance computing technologies together with high-resolution earthquake model will enable us for simulating strong ground motion near future.

[49] The Hoei earthquake, extending as it did from Suruga Bay to Hyuga-nada, approximately 700 km, broke five fault segments (N1–N5′), each with a different geometry. The linkage process between different subfaults in Nankai Trough earthquakes may contribute significantly to the severity of the disaster, especially the tsunamis. Some researchers have claimed that delayed rupture between subfaults amplifies tsunami height over a wide area due to overlap of individual tsunamis from different fault segments [*Kawata et al.*, 2003; *Imai et al.*, 2010]. Moreover, an unusual earthquake with very slow fault rupture speed (e.g., Vr < 0.2 km/s) which is almost comparable to the tsunami propagation speed in deep (e.g., h > 4000 m) sea might amplify tsunami along the direction of fault rupture propagation due to the rupture directivity effect. Such earthquakes with very slow rupture speeds may not produce strong ground motions or large shaking intensity to feel peoples. The contrast of larger tsunami relative to weaker ground shaking raises the potential for a significant tsunami disaster similar to that of the tsunami earthquakes [e.g., *Kanamori*, 1972; *Satake and Tanioka*, 1999].

[50] *Baba et al.* [2006] revealed from tsunami data that the area of large tsunami generation on the fault plane extended along the entire source rupture area in of the 1946 Nankai earthquake. *Sagiya and Thatcher* [1999] also obtained similar source rupture pattern using the geodetic data. This area roughly corresponds to the N3 and N4 segments of *An'naka et al.* [2003]. However, another source model for this event based on strong ground motion and teleseismic waveform data shows a large fault slip only in the eastern part (N3) of the Nankai earthquake fault segment [*Murotani*, 2007]. A possible explanation is that slow rupture over the N4 subfault segment generated large coseismic ground deformation and therefore a large tsunami, but did not produce strong ground motion. Existing seismic data would appear to be inadequate to confirm or deny this conjecture, but the possibility of different rupture characteristics on the different subfaults is intriguing. We should be prepared for a diversity of rupture processes during future earthquakes along the Nankai Trough. Finally, this study suggests that earthquake rupture extent along the Nankai Trough may not be as limited as previously described: as combinations of subfaults to produce Nankai, Tonankai, or Tokai earthquakes, or as a grand combination of subfaults N1–N4 to produce a larger earthquake. The Hoei earthquake was a larger event in which rupture spread as far as Hyuga-nada, incorporating the fifth subfault, N5. Such larger events do not occur during the regular Nankai Trough earthquake cycle of 100–150 years, but may occur in a hyperearthquake cycle of 300 to 500 years. The tsunami deposits at Ryujin Lake in Kyushu left by large tsunamis from the 684 Tenmu, 1361 Shohei, and 1707 Hoei earthquakes, attest to such a hyperearthquake cycle.

[51] **Acknowledgments.** We thank two anonymous reviewers and an associate editor for their constructive comments for improving manuscript. This study was supported by the Research Project "Improvements in strong ground motion and tsunami simulation accuracy for application to realistic disaster prevention of Nankai Trough megathrust earthquakes" of the Ministry of Education, Culture, Sports and Technology of Japan. We thank the Central Disaster Mitigation Council, Cabinet Office, government of Japan, and Yonouzu Promotion Office, Oita Prefecture, Japan, for providing bathymetry map data.

References

Aida, I. (1981), Numerical experiments for the tsunamis generated off the coast of the Nankaido district, *Bull. Earthquake Res. Inst.*, *56*, 713–730.

Ando, M. (1975), Source mechanisms and tectonic significance of historical earthquakes along the Nankai Trough, Japan, *Tectonophysics*, *27*, 119–140, doi:10.1016/0040-1951(75)90102-X.

An'naka, T., K. Inagaki, H. Tanaka, and K. Yanagisawa (2003), Characteristics of great earthquakes along the Nankai trough based on numerical tsunami simulation, *J. Earthquake Eng.* [CD-ROM], *27*, article 307.

Baba, T., Y. Tanioka, P. R. Cummins, and K. Uhira (2002), The slip distribution of the 1946 Nankai earthquake estimated from tsunami inversion using a new plate model, *Phys. Earth Planet. Inter.*, *132*, 59–73, doi:10.1016/S0031-9201(02)00044-4.

Baba, T., P. R. Cummins, T. Hori, and Y. Kaneda (2006), High precision slip distribution of the 1944 Tonankai earthquake inferred from tsunami waveforms: Possible slip on a splay fault, *Tectonophysics*, *426*, 119–134, doi:10.1016/j.tecto.2006.02.015.

Chida, N., and F. Nakayama (2006), Time series analysis of the tsunamis caused by Hoei and Ansei Nankai earthquake in Yonouzu, Oita prefecture, east central Kyushu, *Res. Bull. Fac. Educ. Welfare Sci. Oita Univ.*, *29*(1), 69–80.

Chida, N., S. Takamiya, H. Hamada, T. Tomimatsu, and S. Mitarai (2003), Historical materials of the tsunamis in Yonouzu village, southern part of Oita prefecture, southwest Japan, which were caused by earthquakes of October 28, 1707 and November 24, 1854, *Res. Bull. Fac. Educ. Welfare Sci. Oita Univ.*, *26*(1), 129–143.

Cummins, P. R., and Y. Kaneda (2000), Possible splay fault slip during the 1946 Nankai earthquake, *Geophys. Res. Lett.*, *27*, 2725–2728, doi:10.1029/1999GL011139.

Cummins, P. R., T. Hori, and Y. Kaneda (2001), Splay fault and megathrust earthquake slip in the Nankai Trough, *Earth Planets Space*, *53*, 243–248.

Fitch, T. J., and C. H. Scholz (1971), Mechanism of underthrusting in southwest Japan: A model of convergent plate interactions, *J. Geophys. Res.*, *76*, 7260–7292, doi:10.1029/JB076i029p07260.

Goto, C., and Y. Ogawa (1997), *IUGG/IOC TIME PROJECT: Numerical Method of Tsunami Simulation With the Leap-Frog Scheme—Part 1: Shallow Water Theory and Its Difference Scheme, Manuals and Guides*, vol. 35, 43 pp., U. N. Educ., Sci. and Cult. Organ., Paris.

Harada, T., and K. Ishibashi (2006), Consideration of "giant Nankai earthquake" suggested by deposits in a lagoon in Oita prefecture by means of tsunami simulation, paper presented at Fall Meeting, Seismol. Soc. of Jpn., Nagoya, Japan.

Hashimoto, C., T. Sagiya, and M. Matsuura (2009), Interplate coupling in southwest Japan inferred from GPS data inversion, paper presented at Fall Meeting, Seismol. Soc. of Jpn., Kyoto, Japan.

Hatori, T. (1966), Vertical displacement in a tsunami source area and the topography of the sea bottom, *Bull. Earthquake Res. Inst. Tokyo Univ.*, *44*, 1449–1464.

Hatori, T. (1974), Sources of large tsunamis in southwest Japan, *J. Seismol. Soc. Jpn.*, *27*, 10–24.

Hatori, T. (1985), Field investigation of historical tsunamis along the east coast of Kyushu, West Japan, *Bull. Earthquake Res. Inst. Univ. Tokyo*, *60*, 439–459.

Hirose, H., and K. Obara (2005), Repeating short- and long-term slow slip events with deep tremor activity around Bungo channel region, southwest Japan, *Earth Planets Space*, *57*, 961–972.

Ichinose, G. A., H. K. Thio, P. G. Somerville, T. Sato, and T. Ishii (2003), Rupture process of the 1944 Tonankai earthquake (Ms 8.1) from the inversion of teleseismic and regional seismograms, *J. Geophys. Res.*, *108*(B10), 2497, doi:10.1029/2003JB002393.

Ichitani, S., K. Tsuka, and T. Tabei (2010), Spatial variation of slip deficit rate at the Nankai Trough, southwest Japan inferred from three-dimensional GPS crustal velocity fields—Repeated geodetic inversion analyses for the shifted target area, *J. Seismol. Soc. Jpn.*, *2*(63), 35–44.

Imai, K., K. Satake, and T. Furumura (2010), Amplification of tsunami heights by delayed rupture of great earthquakes along the Nankai trough, *Earth Planets Space*, *62*, 427–432, doi:10.5047/eps.2009.12.005.

Ishibashi, K. (1981), Specification of a soon-to-occur seismic faulting in the Tokai district, central Japan, based upon seismotectonics, in *Earthquake Prediction: An International Review*, *Maurice Ewing Ser.*, vol. 31, edited by D. W. Simpson and P. G. Richards, pp. 297–332, AGU, Washington, D. C.

Ishibashi, K. (2004), Status of historical seismology in Japan, *Ann. Geophys.*, *47*(2–3), 339–368.

Kanamori, H. (1972), Tectonic implications of the 1944 Tonankai and the 1946 Nankaido earthquake, *Phys. Earth Planet. Inter.*, *5*, 129–139, doi:10.1016/0031-9201(72)90082-9.

Kawasumi, H. (1950), *Crustal Deformations as Deduced From Mareographic Data*, Comm. for the Synoptic Dev. of the Shikoku District, Tokyo.

Kawata, Y., S. Suzuki, and T. Takahashi (2003), An effect of giant earthquake scenarios at the Nankai trough on a tsunami hazard, *Proc. Coastal Eng. JSCE*, *50*, 326–330.

Komatsubara, J., and O. Fujiwara (2007), Overview of Holocene tsunami deposits along the Nankai, Suruga, and Sagami troughs, southwest Japan, *Pure Appl. Geophys.*, *164*, 493–507, doi:10.1007/s00024-007-0179-y.

Mansinha, L., and D. E. Smylie (1971), The displacement fields of inclined faults, *Bull. Seismol. Soc. Am.*, *61*, 1433–1440.

Matsuoka, H., and M. Okamura (2009), Nankai earthquakes recorded in tsunami sediments during the last 5000 years, *Eos Trans. AGU*, *90*(52), Fall Meet. Suppl., Abstract T33B-1885.

Moore, G. F., N. L. Bangs, A. Taira, S. Kumamoto, E. Pangborn, and H. J. Tobin (2007), Three-dimensional splay fault geometry and implications for tsunami generation, *Science*, *318*, 1128–1131, doi:10.1126/science.ek1147195.

Murakami, H., T. Shimada, S. Itoh, N. Yamamoto, and J. Ishizuka (1996), Reexamination of the heights of the 1606, 1707 and 1854 Nankai tsunamis along the coast of Shikoku Island, *J. Jpn. Soc. Nat. Disaster Sci.*, *15*(1), 39–52.

Murotani, S. (2007), Source process of the 1946 Nankai earthquake estimated from seismic waveforms and leveling data, Ph.D. thesis, Univ. of Tokyo, Tokyo.

Nanayama, F., and K. Shigeno (2004), An overview of onshore tsunami deposits in coastal lowland and our sedimentological criteria to recognize them, in *Earthquake-Induced Event Deposits. From Deep Sea to on Land*, *Mem. of Geol. Soc. of Jpn.*, vol. 58, edited by O. Fujiwara, K. Ikehara, and F. Nanayama, pp. 19–33, Geol. Soc. of Jpn., Tokyo.

Nishimura, S., M. Ando, and S. Miyazaki (1999), Inter-plate coupling along the Nanaki trough and southeastward motion along southern part of Kyushu, *J. Seismol. Soc. Jpn.*, *2*(51), 443–456.

Okamura, M., T. Kurimoto, and H. Matsuoka (1997), Coastal and lake deposits as a monitor, *Chikyu Mon.*, *19*, 469–473.

Okamura, M., H. Matsuoka, E. Tsukuda, and Y. Tsuji (2000), Tectonic movements of recent 10000 years and observations of historical tsunamis based on coastal lake deposits, *Chikyu Mon.*, *28*, 162–168.

Okamura, M., Y. Tsuji, and T. Miyamoto (2003), Seismic activities along Nankai Trough recorded in coastal lake deposits, *Kaiyo Mon.*, *35*, 312–314.

Okamura, M., H. Matsuoka, N. Chida, and K. Shimazaki (2004), Recurrence intervals of super Nankai earthquakes, paper presented at Fall Meeting, Seismol. Soc. Jpn., Fukuoka, Japan.

Omori, F. (1913), *An Account of the Destructive Earthquakes in Japan, Publ. of the Earthquake Invest. Comm.*, vol. 68B, pp. 1–179, Earthquake Invest. Comm., Tokyo.

Sagiya, T., and W. Thatcher (1999), Coseismic slip resolution along a plate boundary megathrust: The Nankai Trough, southwest Japan, *J. Geophys. Res.*, *104*, 1111–1129, doi:10.1029/98JB02644.

Satake, K. (1993), Depth distribution of coseismic slip along the Nankai Trough, Japan, from joint inversion of geodetic and tsunami data, *J. Geophys. Res.*, *98*, 4553–4565.

Satake, K., and Y. Tanioka (1999), Sources of tsunami and tsunamigenic earthquakes in subduction zones, *Pure Appl. Geophys.*, *154*, 467–483, doi:10.1007/s000240050240.

Strasser, M., G. F. Moore, G. Kimura, Y. Kitamura, A. J. Kopf, S. Lallemant, J.-O. Park, E. J. Screaton, X. Su, and M. B. Underwood (2009), Origin and evolution of a splay fault in the Nankai accretionary wedge, *Nat. Geosci.*, *2*, 648–652, doi:10.1038/ngeo609.

Takahashi, T., F. Imamura, and N. Shuto (1993), Numerical simulation of topography change due to tsunamis, paper presented at IUGG/IOC International Tsunami Symposium, Int. Union of Geod. and Geophys., Wakayama, Japan.

Tanioka, Y. (2001), Interpretation of the slip distributions estimated using tsunami waveforms for the 1944 Tonankai and 1946 Nankai earthquakes, *J. Geogr.*, *110*, 491–497.

Tanioka, Y., and K. Satake (2001), Detailed coseimic slip distribution of the 1944 Tonankai earthquake estimated from tsunami waveforms, *Geophys. Res. Lett.*, *28*, 1075–1078, doi:10.1029/2000GL012284.

Tsuji, Y., M. Okamura, H. Matsuoka, and Y. Murakami (1998), Study of tsunami traces in lake floor sediment of the Lake Hamanako, *Hist. Earthquake*, *14*, 101–113.

Tsuji, Y., M. Okamura, H. Matsuoka, T. Goto, and S. S. Han (2002), Prehistorical and historical tsunami traces in lake floor deposits, Oike Lake, Owase City and Suwaike Lake, Kii-Nagashima City, Mie Prefecture, central Japan, *Chikyu Mon.*, *24*, 743–747.

Tsukuda, E., M. Okamura, and H. Matsuoka (1999), Earthquakes of recent 2000 years recorded in geologic strata, *Chikyu Mon.*, *XX*, 64–69.

Usami, T. (1996), Descriptive table of major earthquakes in and near Japan which were accompanied by damages, *Bull. Earthquake Res. Inst. Tokyo Univ.*, *44*, 1571–1622.

Usami, T. (2003), *Materials for Comprehensive List of Destructive Earthquakes in Japan*, Univ. of Tokyo Press, Tokyo.

Yagi, Y., and M. Kikuchi (2003), Partitioning between seismogenic and aseismic slip as highlighted from slow slip events in Hyuga-nada, Japan, *Geophys. Res. Lett.*, *30*(2), 1087, doi:10.1029/2002GL015664.

Yamanaka, Y. (2004), Source process of the 1944 Tonankai and the 1945 Mikawa earthquake, *Chikyu Mon.*, *305*, 739–745.

Yoshioka, S. (2007), Difference in the maximum magnitude of interpolate earthquakes off Shikoku and in the Hyuganada region, southwest Japan, inferred from the temperature distribution obtained from numerical modeling: The proposed Hyuganada triangle, *Earth Planet. Sci. Lett.*, *263*, 309–322, doi:10.1016/j.epsl.2007.08.025.

T. Furumura and T. Maeda, Earthquake Research Institute, University of Tokyo, 1-1-1 Yayoi, Bunkyo-ku, Tokyo 113-0032, Japan. (furumura@eri.u-tokyo.ac.jp)

K. Imai, Tsunami Engineering Laboratory, Disaster Control Research Center, Tohoku University, Sendai 980-8579, Japan.